



A self-powered and self-functional tracking system based on triboelectric-electromagnetic hybridized blue energy harvesting module

Lingxiao Gao^{a,b,1}, Shan Lu^{a,1}, Weibo Xie^c, Xin Chen^{a,b}, Liangke Wu^g, Tingting Wang^h, Aobo Wang^h, Caiqian Yue^h, Daqiao Tong^a, Wenqian Lei^a, Hua Yu^a, Xiaobin Heⁱ, Xiaojing Mu^{a,c,**}, Zhong Lin Wang^{b,d,e,***}, Ya Yang^{b,e,f,*}

^a Key Laboratory of Optoelectronic Technology & Systems Ministry of Education, International R & D Center of Micro-nano Systems and New Materials Technology, Chongqing University, Chongqing, 400044, China

^b CAS Center for Excellence in Nanoscience, Beijing Key Laboratory of Micro-nano Energy and Sensor, Beijing Institute of Nanoenergy and Nanosystems, Chinese Academy of Sciences, Beijing, 100083, China

^c State Key Laboratory of Mechanical Transmissions, Chongqing University, Chongqing, 400044, China

^d School of Material Science and Engineering, Georgia Institute of Technology, Atlanta, GA, 30332-0245, USA

^e School of Nanoscience and Technology, University of Chinese Academy of Sciences, Beijing, 100049, PR China

^f Center on Nanoenergy Research, School of Physical Science and Technology, Guangxi University, Nanning, Guangxi, 530004, PR China

^g College of Aerospace Engineering, Chongqing University, Chongqing, 400044, China

^h China Academy of Aerospace Aerodynamics, Beijing, 100074, PR China

ⁱ Shanghai Academy of Spaceflight Technology, Shanghai Institute of Space Power Source, Shanghai, 200245, China

ARTICLE INFO

Keywords:

Magnetolectric and triboelectric hybridized nanogenerator
Blue energy
Self-powered
Self-functional
Tracking system

ABSTRACT

The position tracking and attitude monitoring are essential for marine equipment's survival in the boundless ocean. The power solution for aforementioned monitoring system became the bottleneck once its own equipped traditional battery pack run out of the power. Hence, a self-powered and self-functional tracking system has been proposed to meet the technique gap, which consists of a triboelectric-functioned inertial module and an electromagnetic powered global position system (GPS) module. A sophisticated-designed rotating gyro structure, together with triboelectric-electromagnetic working principal, established a battery-less tracking system successfully. Specially, the remarkable gyro rolling mode solution of triboelectric nanogenerator (TENG) features its sensitivity, multiple directions and robustness. Finally, the triboelectric-electromagnetic hybridized module was well validated in an autonomous underwater vehicle (AUV) in the Huanghai Sea. This work not only provides an effective and sustainable way toward large-scale blue energy scavenging, but also reveals TENG' promising potential on inertial sensing capability for marine equipment.

1. Introduction

The position tracking and attitude monitoring system of the marine equipment are two crucial factors to ensure their safe navigation in the boundless ocean [1]. The perfect combination of global position system (GPS) and compass provides a promising solution for the tracking system of the marine equipment [2]. As the power is the blood of tracking

systems, a reliable power is the key consideration. Especially, in the search and rescue of marine disasters, the power solution of GPS is particularly important, once its own equipped traditional battery pack run out of the power [3]. It has raised urgent and challenging requirements for portable and sustainable power sources of using nanogenerators instead of Li-ion batteries [4,5]. Among possible environmental energy sources, the blue energy is highly sought-after,

* Corresponding author. CAS Center for Excellence in Nanoscience, Beijing Key Laboratory of Micronano Energy and Sensor, Beijing Institute of Nanoenergy and Nanosystems, Chinese Academy of Sciences, Beijing, 100083, China.

** Corresponding author. Key Laboratory of Optoelectronic Technology & Systems Ministry of Education, International R & D center of Micro-nano Systems and New Materials Technology, Chongqing University, Chongqing, 400044, China.

*** Corresponding author. School of Material Science and Engineering, Georgia Institute of Technology, Atlanta, GA, 30332-0245, USA.

E-mail addresses: mxjacj@cqu.edu.cn (X. Mu), zhong.wang@mse.gatech.edu (Z.L. Wang), yayang@binn.cas.cn (Y. Yang).

¹ These authors contributed equally to this work.

due to its inexhaustible and convenient properties [6]. In spite of tremendous efforts deployed over the years, the commercial applications of ocean energy still faces great challenges, because most of converters for water wave energy exhibit unsatisfactory efficiency and high cost [7–12]. Therefore, a new type of energy capture technology for the blue energy harvesting is an urgent need.

Triboelectric-electromagnetic hybridized mechanism has been demonstrated as an effective approach to realize high output performance for blue energy [13–15]. The triboelectric nanogenerators (TENGs) exhibit high output voltage [16,17], while electromagnetic generators (EMGs) deliver high output current, which can be used as a complementary method [18–20]. Especially, the TENG is not only a new energy technology, but also a promising sensing technology duo to its self-functional ability [21–25]. However, most of converters adopt sliding structure, which reveals high friction resistance and low sensitivity [26,27]. Although some converters based on rolling electrification present high robustness with minimized wearing of materials, they just can roll in a limited direction [28]. Since the vibration motion of the blue energy is irregular and multidirectional, a comprehensive strategy that appropriately hybridizes the TENG and EMG is highly desired for blue energy harvesting [29].

Here, a self-powered and self-functional tracking system based on triboelectric-electromagnetic hybridized blue energy harvesting module has been first demonstrated. The unique rotating gyro design enables the system to scavenge the wave energy of low frequency and irregular vibration high efficiently. The resultant motion of the gyro is consisted of rotation and revolution motion, where triboelectric and electromagnetic energy was generated respectively. In order to evaluate the module dynamic behavior comprehensively, a linear motor platform was established with oscillation frequency, acceleration, and wavelength as test variables. At the same time, its output under different wave frequency and amplitude were also studied, which demonstrated its ability for wave energy harvesting. Furthermore, eight pairs of triboelectric electrodes were designed, from which the motion of the gyro could be monitored through recording the electrification signal. The remarkable

gyro rolling mode solution of triboelectric nanogenerator (TENG) features its robustness, which could be the second-generation technology in rolling mode TENG family. Then combined with the GPS powered by EMG, a self-powered and self-functional tracking system was integrated triumphantly. Finally, its effectiveness towards blue energy harvesting was demonstrated on a buoy in Jialing River and an autonomous underwater vehicle (AUV) in Huanghai Sea, respectively. This work not only provides an effective and sustainable way toward large-scale blue energy harvesting, but also reveals the promising potential of TENG on inertial sensing capability for marine equipment.

2. Results and discussion

2.1. The structure and working principle of the hybridized nanogenerator

A self-powered and self-functional tracking system can be constructed by a magneto-electric and triboelectric hybridized nanogenerator. The TENG extracts the hull vibration energy from the ocean, producing electricity, which is further used to analyze the motion attitude of the marine equipment, while the EMG harvests ocean energy to power the GPS receiver on the marine equipment. To realize such a self-powered and self-functional tracking system, a magneto-electric and triboelectric hybridized nanogenerator based on a gyro structure was designed, as displayed in Fig. 1b, which is mainly consists of a white resin gyro, six coils, a cylindrical NdFeB magnet, two triboelectric electrodes, a cylindrical frame and some connecting parts. The cylindrical frame was made by 3D printing technology, and its inner diameter and height were 110 mm and 40 mm, respectively. Six groups of coils were evenly spaced on the sidewall of the cylindrical frame, and each had a dimension of $\Phi 35 \text{ mm} \times 5 \text{ mm}$. The cylindrical magnet with a dimension of $\Phi 18 \text{ mm} \times 20 \text{ mm}$ was embedded in the white resin gyro. Meanwhile, a piece of fluorinated ethylene propylene (FEP) triboelectric film was attached on the outer surface of the white resin gyro. Lastly, a printed circuit board (PCB) coated with an equidistant tin layer was attached to the bottom of the cylindrical frame as the triboelectric

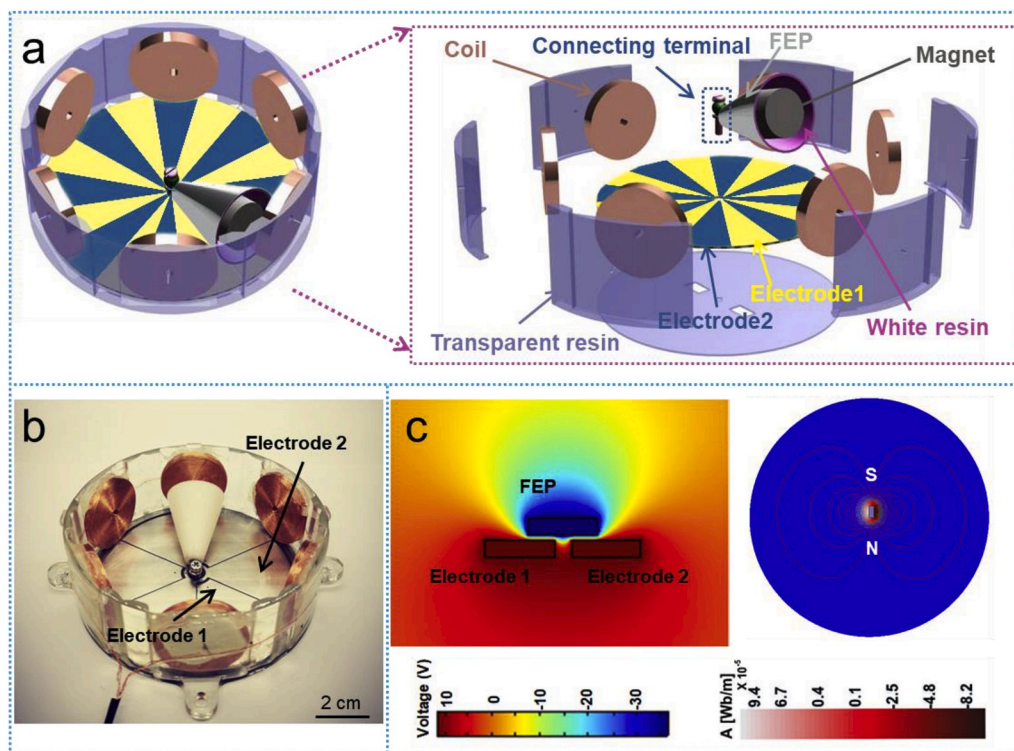


Fig. 1. Structure and working principle of the hybridized nanogenerator. a) The structure of the hybridized nanogenerator. b) Digital photograph of the hybridized nanogenerator. c) The simulated map of the TENG based on the COMSOL software and the simulated map of the EMG based on the Maxwell 15.0 software.

electrodes (Φ 100 mm). A connecting ring (height of 5 mm) was built into the tip of the cone to realize the rolling motion of the gyro on the PCB board, as depicted in Figure S1a (Supporting Information), and its partial enlarged view is shown in Figure S1b (Supporting Information). The connection ring was nested in on a screw with a dimension of Φ 3 mm \times 25 mm to realize the connection between the gyro and the cylindrical frame. To reduce the friction, a ball (Φ 4.5 mm) with a middle hole (Φ 3.5 mm) was placed between the connecting ring and the screw. The digital photograph of the hybridized nanogenerator is illustrated in Fig. 1c. To theoretically predict the distribution of the electrical potential between the adjacent electrodes of TENG, finite element method analysis was conducted by using COMSOL software, as depicted in Fig. 1d. While Maxwell 15.0 software was used to theoretically predict the flux line distribution of the magnet, which is also displayed in Fig. 1d. The rolling track of the gyro inside the cylindrical frame is presented in Figure S1c (Supporting Information), which took counterclockwise motion as an example. The inter-digital electrode and the grating electrode were designed to characterize the energy capture and sensing capability of the TENG respectively, as illustrated in Figure S1d and Figure S1e (Supporting Information).

In order to avoid mutual interference between the respective outputs, the output of each coil of the EMG first passed through a full-wave rectifier bridge, and then the multi-channel rectified output was connected in parallel, as demonstrated in Figure S2a (Supporting Information).

The inter-digital electrodes and the grating electrodes were designed to characterize the energy capture and sensing capability of the TENG respectively. The electrical connection of TENG with the inter-digital electrodes was illustrated in Figure S2b (Supporting Information). The 360° electrode was divided into 6 parts and the spaced parts were connected separately. The electrical connection of TENG with the grating electrodes was demonstrated in Figure S2c (Supporting Information). The 360° electrode was divided into 16 parts, and the adjacent electrodes were one unit. Lastly, the output of each unit was connected to the data acquisition device respectively.

The type of the TENG can be equivalent to the triboelectric effect between a freestanding dielectric layer such as FEP and several metal electrode pairs (Tin), which serve not only as the triboelectric layers, but also as two electrodes [30]. Taking a pair of electrodes as an example, the triboelectric effect process could be analyzed as Figure S3a (Supporting Information). When the gyro rolled over electrode 1, net opposite charges would be accumulated on FEP film and electrode 1 [31] (Figure S3a-I). Then, when the gyro rolled towards the electrode 2 (Figure S3a-II), the positive charges in the loop would flow from electrode 1 to the electrode 2, resulting in the first half cycle of electricity generation. When the gyro reached the overlapping position of the electrode 2 (Figure S3a-III), all of the positive charges would be driven to the electrode 2. Subsequently, a rolling away from electrode 2 of the gyro would drive the flow of the positive charges from electrode 2 to electrode 1, forming a reverse current in the load (Figure S3a-IV). This is the second half of electricity generation process. During the rolling process, a periodic alternating current (AC) will be generated.

Simultaneously, as the magnet rolled with the gyro, the flux inside the coils would change, which would induce current in the coils to generate a magnetic field, and it would impede the change of the magnetic flux due to the Lenz's law, as illustrated in Figure S3b (Supporting Information). The initial state was when the magnet was facing the coil, and assuming that there was no current in the coil (Figure S3b-I). As the magnet moved away from the coil, the flux line passing through it would decrease, resulting in a clockwise current (Figure S3b-II). When it rolled far enough, there was no magnetic flux inside the coil. So no current could be generated (Figure S3b-III). When the magnet approached the coil again, a counterclockwise current would be generated inside the coil to balance the flux change (Figure S3b-IV).

2.2. Performances of the hybridized generator

The dynamic behavior evaluation of the hybridized nanogenerator was performed on a linear motor platform and the effects of oscillation frequency, acceleration, and wavelength on the outputs were systematically studied, as displayed in Fig. 2. The outputs of six sets of coils connected in parallel after rectifying were studied, as demonstrated in Fig. 2a. The output voltages for EMG part increase from 2.22 to 3.86 V, and the peak values of short circuit current similarly vary from 9.16 to 12.9 mA with the frequency ranging from 1.2 to 2.3 Hz, exhibiting a distinctly increasing trend with the increase of frequency, which should be attributed to the increase of the time-rate variation of magnetic flux linkage. The results are consistent with the Faraday's law [32], which can be given as follows:

$$V = -N \frac{d\Phi}{dt} \quad (1)$$

where V is the induced electromotive force generated in the coil and Φ is the total magnetic flux linkage in one turn of the coil. N and t are the number of the coil's turns and time respectively. Regarding the proposed EMG that consists of a stationary coil and a movable magnet, the V in the coil can be further expressed as

$$V = -N \frac{d\Phi}{dt} = -NS \frac{dB(x)}{dt} = -NS \frac{dB(x)}{dx} \frac{dx}{dt} = -NS \frac{dB(x)}{dx} v \quad (2)$$

where $B(x)$ and S represent the magnetic flux density through the coil and the area of the coil respectively, and v is the velocity of the magnet.

Let's say it was moving at a constant speed, for the designed structure, the angular velocity (ω) can be expressed as

$$\omega = \frac{v}{r} \quad (3)$$

So the frequency (f) is

$$f = \frac{1}{T} = \frac{1}{2\pi/\omega} = \frac{\omega}{2\pi} = \frac{v}{2\pi r} \quad (4)$$

T and r represent period and length of generatrix respectively. Based on Equations (2) and (4), the relation between voltage and frequency can be deduced.

$$V = -NS \frac{dB(x)}{dx} 2\pi r f \quad (5)$$

When the internal resistance of the coil is R_{coil} , the short circuit current generated in the coil can be expressed as

$$I = \frac{V}{R_{coil}} = -\frac{NS}{R_{coil}} \frac{dB(x)}{dx} 2\pi r f \quad (6)$$

So, both of the output voltages and the short circuit currents show positive correlations with the oscillation frequency.

The energy capture capability was characterized by the inter-digital electrodes. Differently, for the TENG part, both of the output voltages and the short circuit currents exhibited a slightly increasing trend with the increase of frequency, while when the frequency was high, they show a slight decrease, as presented in Fig. 2b. Based on the theory of Maxwell's equations [33], the external current of the TENG can be expressed as

$$I = A \frac{d\sigma}{dt} \quad (7)$$

A and σ represents effective contact area and surface charge density respectively. A high output of TENG requires that the two surfaces of triboelectric materials should be fully contacted. Hence, too high rotation speed will reduce the effective contact area, though the output is positively correlated with the frequency.

By adjusting the motion stroke of the linear motor, the effect of water wavelength on the outputs was simulated, as illustrated in Fig. 2c-d.

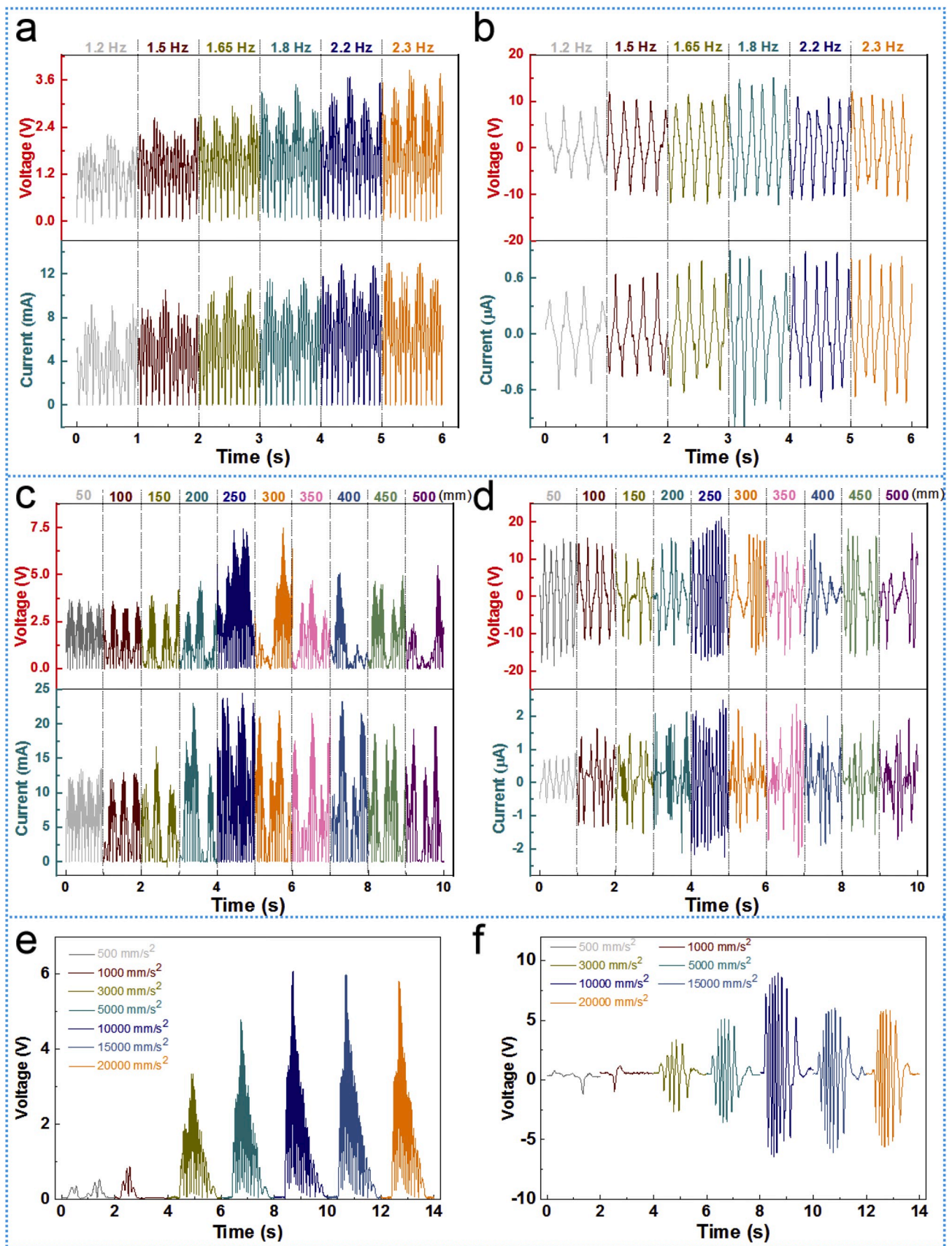


Fig. 2. The outputs of the hybridized nanogenerator on a linear motor. a) The outputs of the EMG in different frequencies. b) The outputs of the TENG in different frequencies. c) The outputs of the EMG in different wavelengths. d) The outputs of the TENG in different wavelengths. e) The outputs of the EMG in different accelerations. f) The outputs of the TENG in different accelerations.

Fig. 2c and d display the outputs of the EMG and TENG, respectively. When the motion stroke ranged from 50 to 200 mm, the device was in the state of primary resonance (movie S1, Supporting Information), so both of the outputs of the EMG and TENG changed slightly. When the motion stroke was 250 mm, the device entered a secondary resonance state, and both of the outputs of the EMG and TENG exhibited a tremendous improvement (movie S2, Supporting Information), which can be attributed to the increase of rolling frequency and tangential pressure. Detailed output waveform of primary resonance and secondary resonance are illustrated in Figure S4 (Supporting Information). However, when the stroke exceeded 250 mm, the motion state of the device was disordered (movie S3, Supporting Information), so the outputs were also disordered.

Supplementary data related to this article can be found at <https://doi.org/10.1016/j.nanoen.2020.104684>.

The outputs were also characterized under different initial acceleration as illustrated in Fig. 2e and f. In Fig. 2e, when the initial acceleration ranged from 500 mm/s^2 to 20000 mm/s^2 , the output voltages of EMG exhibited an increasing trend with the increase of initial acceleration at the beginning and it became constant eventually. This is because a relatively large acceleration increases the gyro speed, and when the acceleration reaches a certain value, the gyro speed reaches the limit. In Fig. 2f, the output voltages of the TENG increased at the beginning and then decreased with the increase of the initial acceleration. This is because when the speed of the gyro reached its limit, the gyro and the

bottom electrode cannot completely contact, thus reducing the effective friction area.

The hybridized generator for energy scavenging in water waves was demonstrated in Fig. 3. Fig. 3a shows the output voltages of TENG measured at wave height range from 20 mm to 125 mm under the frequency of 1.0 Hz. The output voltages of the TENG were found to precisely follow the variation of water height, and its peak to peak voltage increased from 6.5 V to 23.76 V by increasing wave height from 20 mm to 125 mm. A similar trend had been observed in the output voltages of EMG, and a peak to peak voltage increased from 0.75 V to 3.1 V when the wave height increased from 20 mm to 125 mm as presented in Fig. 3b. Fig. 3c–d shows the output voltages of the hybridized generator measured at the frequency range from 0.7 Hz to 1.4 Hz at the wave height of 110 mm. It was found that the resonance frequency of the device could be reached only at the water wave frequency of 1 Hz, and the peak voltages of 11.15 V and 3.1 V were achieved for the TENG and the EMG respectively. While at other frequencies, both of the output of the TENG and the EMG were very low. Additionally, the outputs under wave rising up and wave falling down were also studied which are illustrated in Figure S5a–b (Supporting Information). Furthermore, a simple buoy was made to implant the device and was putted into the Jialing River for testing as displayed in Fig. 3c. Movie S4 (Supporting Information) shows the outputs of the EMG while movie S5 (Supporting Information) is the outputs of the TENG. The peak voltages of 0.65 V and 0.9 V were achieved for the TENG and the EMG, respectively, under

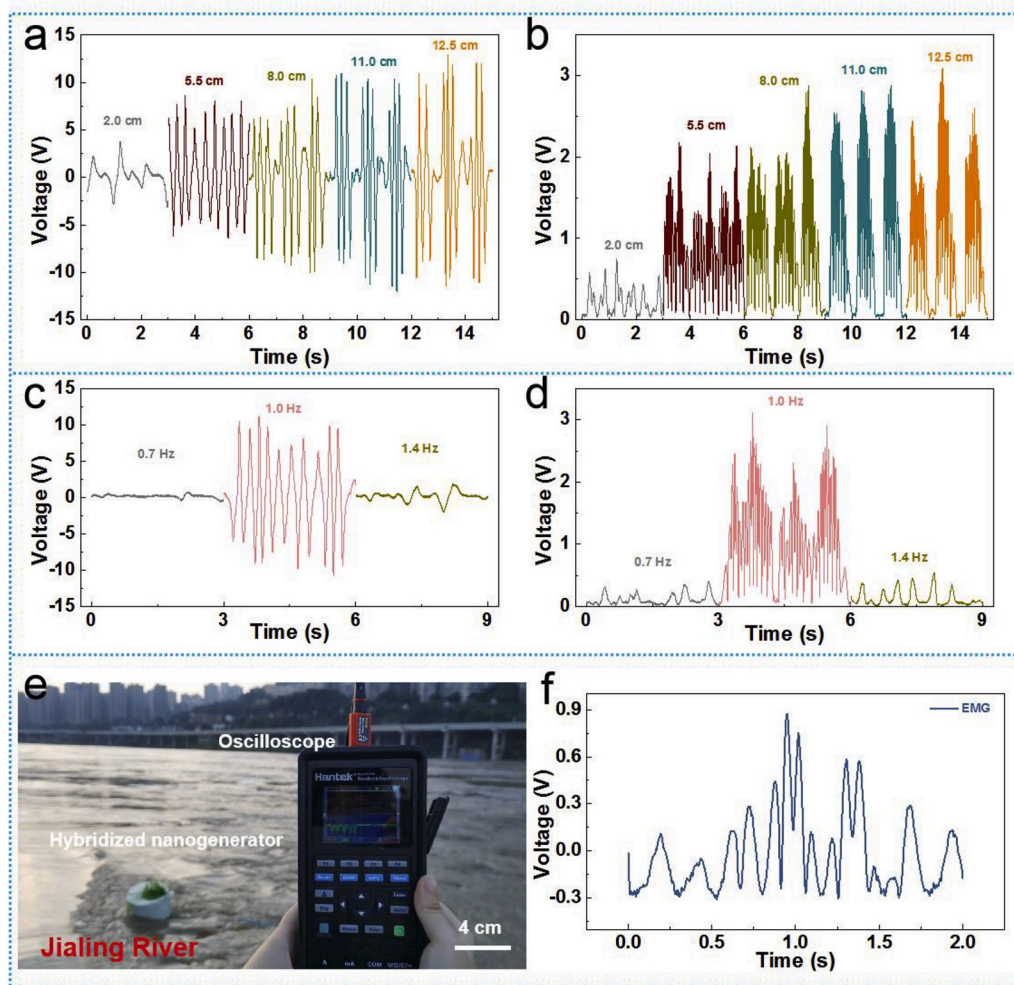


Fig. 3. The output of the hybridized nanogenerator in the water wave. a) The outputs of the TENG in different wave heights. b) The outputs of the EMG in different wave heights. c) The outputs of the TENG in different water wave frequencies. d) The outputs of the EMG in different water wave frequencies. e) The floating buoy hybridized nanogenerator for water wave energy harvesting in Jialing river. f) The outputs of the EMG in Jialing river.

irregular and complicated water waves, as depicted in Fig. 3d and Figure S5c (Supporting Information).

Supplementary data related to this article can be found at <https://doi.org/10.1016/j.nanoen.2020.104684>.

In order to further verify the energy capture capacity of the hybridized generator, the output voltages of TENG were measured with external loads from 1 M Ω to 1000 M Ω , as depicted in Figure S6a (Supporting Information), and a peak output power of 4.1 μ W was achieved under a loading resistance of 10 M Ω . Simultaneously, the output voltages of EMG were measured with external loads from 10 Ω to 1 M Ω , and a peak output power of 14.9 mW was achieved under a loading resistance of 220 Ω , as displayed in Figure S6b (Supporting Information).

2.3. The self-functional navigation system based on TENG

Based on the above analysis, the EMG demonstrated superior energy capture performance, however the TENG was barely satisfactory. Fortunately, it had been demonstrated that the TENGs have excellent sensing capabilities. So, it was employed as a self-functional posture sensing in the future experiments.

A toy car was employed to simulate the motion of the marine equipment such as ships, and the TENG and EMG were used to detect its different movement states, as illustrated in Fig. 4a–c. Fig. 4a is the outputs of the TENG and EMG when the car started, while Fig. 4b and c illustrate the states of starting-braking and starting-swinging-braking, respectively. As compared with the EMG, the TENG shows a higher resolution and sensitivity in attitude monitoring.

In order to improve the sensing function of TENG, the 360° electrode was optimized into eight pairs (Figure S5d, Supporting Information), and the movement monitoring of the ship was realized through analyzing the output phase of eight TENG units. In other words, each unit can be monitored an angle of 45°. To monitor the acceleration of the hull, the TENG was attached onto a substrate connected to the linear motor, and it was characterized by eight channels (Ch1–Ch8) as shown in Figure S5d (Supporting Information). When different accelerations were given in the direction tangent to Ch1, the outputs of the eight channels are shown Fig. 4d. When the acceleration was 500 mm/s², the output order of the eight channels is Ch1–Ch8–Ch7 in sequence, and other channels have no output signal. It's worth noting that the Ch7 had only half a cycle signal. Therefore, the gyro rotates clockwise by 157.5°, which can be deduced from the number of output peaks and the sequence of outputs. Similarly, the direction and angle of the rotation can be derived at other accelerations, as shown in Fig. 4d.

The device was put on the toy car according to the position of Ch7 on the front and Ch3 on the rear to simulate the motion of the marine equipment such as ships. From Fig. 4e, it can be seen that when the ship in the pitching motion, Ch3, Ch4, Ch6 and Ch7 would create vibration signals, while when the ship in the rocking motion, Ch1, Ch5, Ch6 and Ch8 would create vibration signals. At the same time, the turning direction of the ship can be achieved by analyzing the phase of the signals. Movie S6 (Supporting Information) exhibits the monitoring system.

Supplementary data related to this article can be found at <https://doi.org/10.1016/j.nanoen.2020.104684>.

2.4. The self-powered and self-functional navigation system

A series of experiments had been conducted to demonstrate the capability of the self-powered and self-functional navigation system. Fig. 5a displays the 1000 μ F capacitor was charged from 0 V to 3 V in about 6 s by the EMG. The output of the EMG is an alternating current that changes instantaneously, to make use of this power normally, it needs to convert it into a stable DC voltage. However, in consideration of larger load, in case that the output of the MEG is not enough to supply the load continuously, the energy is needed to be stored until the electricity accumulates enough. Therefore, the power management circuit will mainly implement AC-DC conversion, DC voltage regulation, power

storage and release control. The circuit design is illustrated in Fig. 5b. The output power of the EMG was first conditioned by the power management circuit, then stored in a rechargeable lithium battery, and last could be released to a GPS module for power supply. The GPS module then communicated with some satellites to get position information and sent it to a laptop.

The output of each coil of the EMG first passed through a full-wave rectifier bridge, and then the multi-channel rectified output was connected in parallel to a capacitor, which played as a preliminary energy buffer and voltage regulator. Such an independent rectifying structure effectively avoided mutual interference between the respective outputs, which may cause energy loss while collecting the multiple outputs together. The core management component was ADI's specialized energy harvesting power management IC LTC3106, which contained a Buck-Boost DC/DC converter and energy storage management that controlled the energy harvester to charge a rechargeable battery when the energy source was sufficient. When the energy was insufficient, the rechargeable battery supplied the load. With the help of the charging protection function, we could charge the battery until its voltage increased to 4 V, and discharged the battery before its voltage decreased to 3 V, thus protecting the battery from irreversible damage. The DC regulated output voltage was configured for a fixed 3.3 V that could supply a peak current up to 100 mA. The front and back photographs of the management circuit are depicted in Figure S7a–b (Supporting Information). The GPS module was a mass-produced module (NEO-6M), once powered up, it could automatically search and establish contact with the GPS satellite to obtain the current GPS signal, which was sent to a PC and displayed by the software, as displayed in Fig. 5c and movie S7 (Supporting Information). The experiment proves that under the operating conditions of a motor stroke of 50 mm and an acceleration of 1000 m/s², the EMG worked to charge a 80 mAh rechargeable battery continuously for 26 h, then could drive the GPS module to work continuously for 30 min at a transmitting frequency of 1 time per second and a working current of 70 mA.

Supplementary data related to this article can be found at <https://doi.org/10.1016/j.nanoen.2020.104684>.

Lighting LED experiments were carried out on the linear motor and water respectively. As depicted in Fig. 5d and movie S8–9 (Supporting Information), 100 LEDs can be lighted up simultaneously by the EMG. Lastly, the self-powered and self-functional tracking system based on magneto-electric and triboelectric hybridized nanogenerator was well validated in an AUV in Huanghai Sea as demonstrated in Fig. 5e. A data collection and storage system based on STM32F1 was developed to record the outputs of the hybridized nanogenerator in real time as illustrated in Fig. 5f and Figure S7c (Supporting Information). Fig. 5e depicts that the EMG demonstrated superior energy capture performance in the AUV while Fig. 5f displays the TENG could monitor the running status of AUV commendably. For example, the AUV oscillated at 0–8 s and it was tilted at 8–9 s. But it can run more smoothly in 10–13 s.

3. Conclusion

In summary, a self-powered and self-functional tracking system based on triboelectric-electromagnetic hybridized blue energy harvesting module was developed theoretically and experimentally. With the design of rotating gyro structure, a high sensitive energy capture is realized under low frequency and irregular wave vibration. Based on a linear motor platform and a wave pump, the influences of oscillation frequency, acceleration, and wavelength were systematically investigated, which well demonstrated the ability of the nanogenerator for wave energy harvesting. Furthermore, eight pairs of triboelectric electrodes were designed, from which the motion of the gyro could be monitored through recording the electrification signal. The remarkable gyro rolling mode solution of triboelectric nanogenerator (TENG) features its robustness, which could be the second-generation technology in rolling mode TENG family. Then combined with the GPS powered by

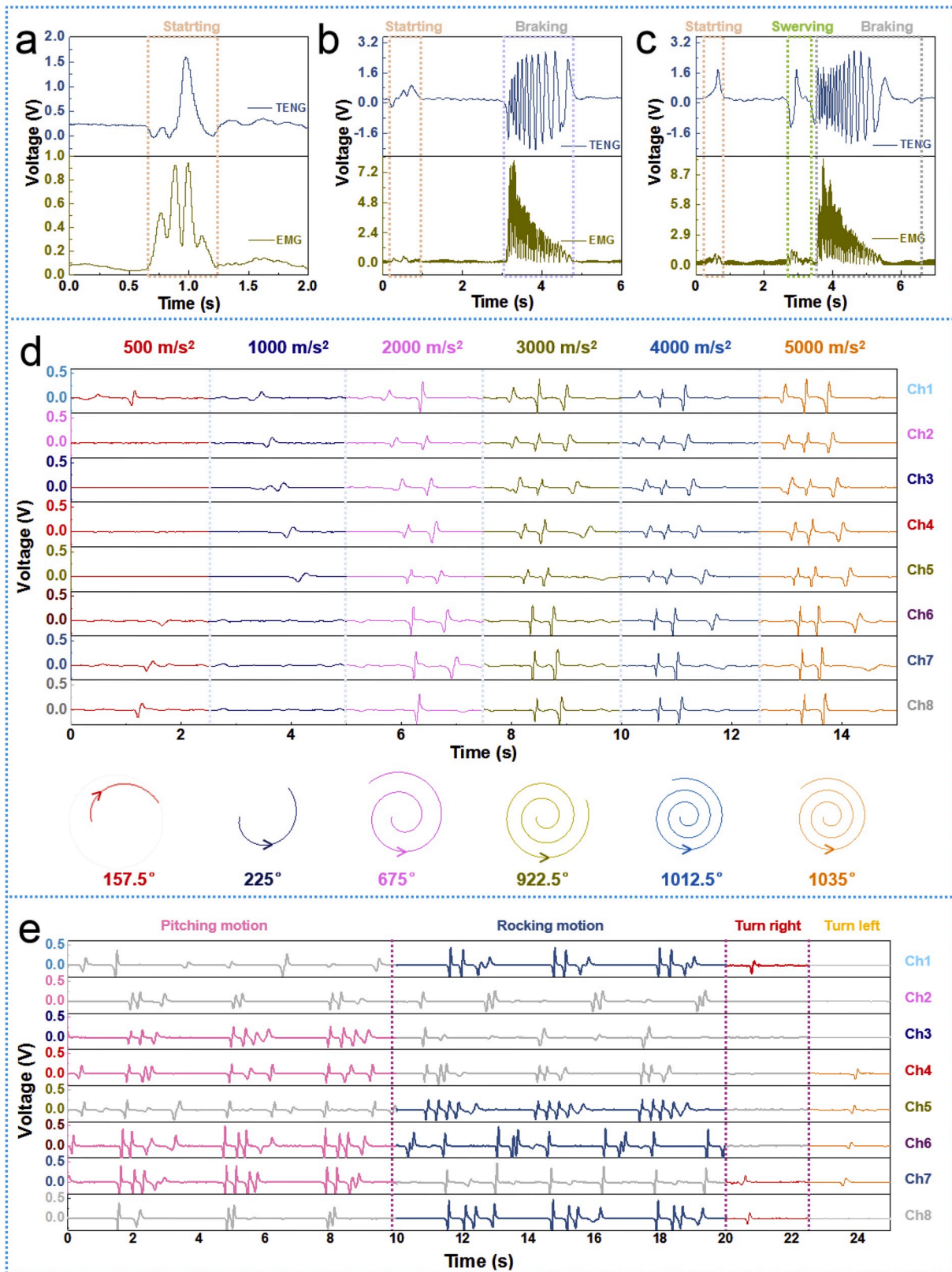


Fig. 4. The self-functional tracking system based on TENG. a) The outputs of the TENG and EMG when the car started. b) The outputs of the TENG and EMG when the car in the states of starting-braking. c) The outputs of the TENG and EMG when the car in the states of starting-swerving-braking. d) The gyro rotation direction and rotation angle at difference accelerations. e) The movement monitoring data based on TENG.

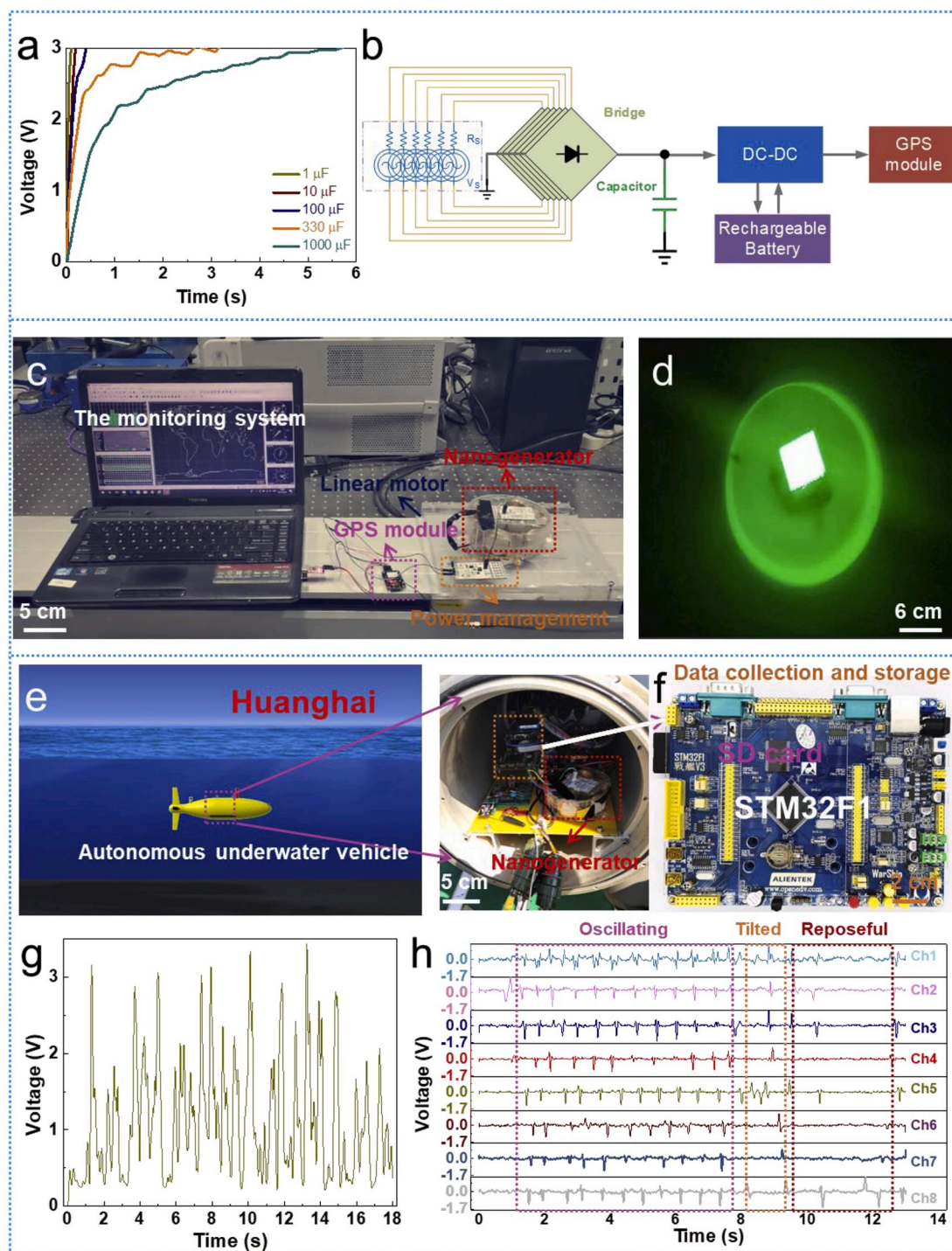


Fig. 5. The self-powered and self-functional tracking system. a) The charge time of the EMG for different capacitors. b) Schematic diagram of the self-powered GPS system. c) Photograph of the self-powered GPS system. e) Schematic diagram of the self-powered and self-functional tracking system validated in an AUV in Huanghai. f) Photograph of the data acquisition and storage system. g) The outputs of the EMG in AUV. h) The outputs of the TENG in AUV.

EMG, a self-powered and self-functional tracking system was integrated triumphantly. Finally, its effectiveness towards blue energy harvesting was demonstrated on a buoy in Jialing River and an autonomous underwater vehicle (AUV) in Huanghai Sea, respectively. This work is not only a paradigm towards large-scale blue energy harvesting, but also overcomes a bottleneck problem towards the power solution of tracking system.

4. Experimental section

Fabrication of the hybridized nanogenerator: The hybridized nanogenerator was fabricated through 3D-printing technology. The hybridized nanogenerator mainly included a gyro which made of white resin (Φ 25 mm \times 40 mm), six coils (Φ 35 mm \times 5 mm), a cylindrical NdFeB magnet (Φ 18 mm \times 20 mm), a triboelectric electrode (Φ 100 mm), a cylindrical frame and (Φ 110 mm \times 40 mm) some connecting parts. The gyro, cylindrical frame and coupling link were fabricated through 3D-

printing technology. A PCB coated with an equidistant tin layer was attached to the bottom of the cylindrical frame as the triboelectric electrode and a piece of FEP film was attached on the outer surface of the white resin gyro as the triboelectric layer. The magnet was embedded in the gyro using hot glue and six equally spaced coils spaced on the inner wall of the cylindrical frame. The gyro was fixed on the center of the cylindrical frame with screws and nuts. To reduce the friction, a ball (Φ 4.5 mm) with a middle hole (Φ 3.5 mm) was placed between the connecting ring and the screw.

Construction of GPS system: The outputs of the EMG were connected to the power end of the GPS system successively after passing the rectifier bridge (MBD54), thin film lithium battery (80 mAh) and DC-DC circuit (LTC3106). Then the data were transmitted to a computer via a serial port for real-time monitoring.

Construction of offshore test platform: The outputs of the hybridized nanogenerator were connected to a development board (STM32F103) which was used for data collection and storage. The whole equipment was installed in the AUV compartment which was developed by China Academy of Aerospace Aerodynamics. At the end of the test, the data was read to the computer for analyzing and processing.

Electrical measurement and characterization: The short-circuit currents of the hybridized nanogenerator were acquired by a programmable electrometer (Keithley model 6514) and a Data Acquisition Card (NI PCI-6259) on a Desktop PC. The output voltage data (Fig. 2, Figure S4 and Fig. 4a–c) excited by linear motor (DGL200-AUM4) were acquired by an oscilloscope (MSO2024B). The output voltage data (Fig. 3a–d and Figure S5a–b) excited by wave pump (CX-W3 (II)) were acquired by a hand-held oscilloscope (Hantek 2C42). The output voltage data (Fig. 4d–e) were acquired by two oscilloscope (MSO2024B and MSOX3024T).

Declaration of competing interest

The authors declare no conflict of interest.

CRediT authorship contribution statement

Lingxiao Gao: Conceptualization, Data curation, Writing - original draft, Visualization. **Shan Lu:** Conceptualization, Data curation, Writing - original draft, Visualization. **Weibo Xie:** Conceptualization, Data curation, Writing - original draft, Visualization. **Xin Chen:** Formal analysis, Resources, Validation. **Liangke Wu:** Software, Visualization. **Tingting Wang:** Formal analysis, Resources, Validation. **Aobo Wang:** Formal analysis, Resources, Validation. **Caiqian Yue:** Formal analysis, Resources, Validation. **Daqiao Tong:** Software, Visualization. **Wenqian Lei:** Software, Visualization. **Hua Yu:** Software, Visualization. **Xiaobin He:** Software, Visualization. **Xiaojing Mu:** Funding acquisition, Project administration, Supervision, Writing - review & editing. **Zhong Lin Wang:** Funding acquisition, Project administration, Supervision, Writing - review & editing. **Ya Yang:** Funding acquisition, Project administration, Supervision, Writing - review & editing.

Acknowledgements

This work was supported by the National Key Research and Development Program of China (Grant No. 2016YFB0402702, Grant No. 2016YFA0202701), National Natural Science Foundation of China (Grant No. 51605060, Grant Nos. 51472055), the Fundamental Research Funds for the Central Universities (No. 2018CDPTCG0001-5), the Chongqing municipality key research and development program of china (Grant No. cstc2017rgzn-zdyfX0041), the Research Funds from Shanghai Institute of Space Power-source (YF07050118F5655), External Cooperation Program of BIC, Chinese Academy of Sciences (Grant No. 121411KYS820150028), the 2015 Annual Beijing Talents Fund (Grant No. 2015000021223ZK32), Qingdao National Laboratory for Marine Science and Technology (No. 2017ASKJ01), and the

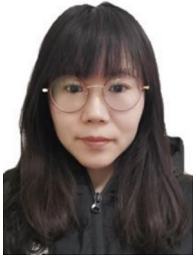
University of Chinese Academy of Sciences (Grant No. Y8540XX2D2), Chongqing Venture & Innovation Support Program for Chongqing Overseas Returnees, Science and Technology on Analog Integrated Circuit Laboratory (Grant No.614280201140117), National Natural Science Foundation of China of China (Grant No.61874015) and The National Key Research and Development Program of China (Grant No.2018YFC0117202), The Fund for cultivating talent of Chongqing University (CQU2019HBRC1A04).

Appendix A. Supplementary data

Supplementary data to this article can be found online at <https://doi.org/10.1016/j.nanoen.2020.104684>.

References

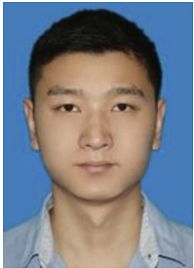
- [1] K.Y. Pettersen, O. Egeland, IEEE Trans. Automat. Contr. 44 (1999) 112–535.
- [2] M. Ueno, J. Mar. Sci. Technol. 5 (2000) 9–15.
- [3] L.X. Gao, D.L. Hu, M.K. Qi, J. Gong, H. Zhou, X. Chen, J.F. Chen, J. Cai, L.K. Wu, N. Hu, Y. Yang, X.J. Mu, Nanoscale 10 (2018) 19781.
- [4] Y. Bai, L. Xu, C. He, L.P. Zhu, X.D. Yang, T. Jiang, J.H. Nie, W. Zhong, Z.L. Wang, Nano Energy 66 (2019) 104117.
- [5] F.B. Xia, Y.K. Pang, G.X. Liu, S.W. Wang, W. Li, C. Zhang, Z.L. Wang, Nano Energy 61 (2019) 1–9.
- [6] J. Tollefson, Nature 508 (2014) 302–304.
- [7] J. An, Z.M. Wang, T. Jiang, X. Liang, Z.L. Wang, Adv. Funct. Mater. 29 (2019) 1904867.
- [8] G.L. Liu, H.Y. Guo, S.X. Xu, C.G. Hu, Z.L. Wang, Adv. Energy Mater. 9 (2019) 1900801.
- [9] M.Y. Xu, T.C. Zhao, C. Wang, S.L. Zhang, Z. Li, X.X. Pan, Z.L. Wang, ACS Nano 13 (2019) 1932–1939.
- [10] X. Liang, T. Jiang, G.X. Liu, T.X. Xiao, L. Xu, W. Li, F.B. Xi, C. Zhang, Z.L. Wang, Adv. Funct. Mater. 29 (2019) 1807241.
- [11] J.Y. Wang, L. Pan, H.Y. Guo, B.B. Zhang, R.R. Zhang, Z.Y. Wu, C.S. Wu, L.J. Yang, R.J. Liao, Z.L. Wang, Adv. Energy Mater. 9 (2019) 1802892.
- [12] X.Y. Li, J. Tao, X.D. Wang, J. Zhu, C.F. Pan, Z.L. Wang, Adv. Energy Mater. 8 (2018) 1800705.
- [13] H. Guo, Z. Wen, Y. Zi, M. Yeh, J. Wang, L. Zhu, C. Hu, Z.L. Wang, Adv. Energy Mater. 6 (2016) 1501593.
- [14] Z. Wen, H. Guo, Y. Zi, M. Yeh, X. Wang, J. Deng, J. Wang, S. Li, C. Hu, L. Zhu, Z. L. Wang, ACS Nano 10 (2016) 6526–6534.
- [15] H. Shao, P. Cheng, R. Chen, L. Xie, N. Sun, Q. Shen, X. Chen, Q. Zhu, Y. Zhang, Y. Liu, Z. Wen, X. Sun, Nano-Micro Lett. 10 (2018) 54.
- [16] L.X. Gao, X. Chen, S. Lu, H. Zhou, W.B. Xie, J.F. Chen, M.K. Qi, H. Yu, X.J. Mu, Z. L. Wang, Y. Yang, Adv. Energy Mater. 10 (2019) 1902725.
- [17] S. Wang, X. Mu, Y. Yang, C. Sun, A. Gu, Z.L. Wang, Adv. Mater. 27 (2015) 240–248.
- [18] C. Saha, T. Donnell, N. Wang, P. McCloskey, Sensor Actuator Phys. 147 (2017) 248–253.
- [19] E. Koukharenko, S. Beeby, M. Tudor, N. White, T. Donnell, C. Saha, S. Kulkarni, S. Roy, Microsyst. Technol. 12 (2006) 1071–1077.
- [20] P. Grishchuk, Physics 6 (2003), 0306013.
- [21] Z.Y. Wu, B.B. Zhang, H.Y. Zou, Z.M. Lin, G.L. Liu, Z.L. Wang, Adv. Energy Mater. 9 (2019) 1901124.
- [22] X.Q. Zhang, M. Yu, Z.R. Ma, H. Ouyang, Y. Zou, S.L. Zhang, H.K. Niu, X.X. Pan, M. Y. Xu, Z. Li, Z.L. Wang, Adv. Funct. Mater. 29 (2019) 1900327.
- [23] J.B. Yu, X.J. Hou, M. Cui, S.N. Zhang, J. He, W.P. Geng, J.L. Mu, X.J. Chou, Nano Energy 64 (2019) 103923.
- [24] K.Y. Meng, J. Chen, X.S. Li, Y.F. Wu, W.J. Fan, Z.H. Zhou, Q. He, X. Wang, X. Fan, Y.X. Zhang, J. Yang, Z.L. Wang, Adv. Funct. Mater. 29 (2019) 1806388.
- [25] X.J. Pu, H.Y. Guo, Q. Tang, J. Chen, L. Feng, G.L. Liu, X. Wang, Y. Xi, C.G. Hu, Z. L. Wang, Nano Energy 54 (2018) 453–460.
- [26] C. Hou, T. Chen, Y. Li, M. Huang, Q. Shi, H. Liu, L. Sun, C. Lee, Nano Energy 63 (2019) 103871.
- [27] X.J. Zhao, S.Y. Kuang, Z.L. Wang, G. Zhu, ACS Nano 12 (2018) 4280–4285.
- [28] L. Lin, Y.N. Xie, S.M. Niu, S.H. Wang, P.K. Yang, Z.L. Wang, ACS Nano 9 (2015) 922–930.
- [29] Z.L. Wang, T. Jiang, L. Xu, Nano Energy 39 (2017) 9–23.
- [30] S.H. Wang, Y.N. Xie, S.M. Niu, L. Lin, Z.L. Wang, Adv. Mater. 26 (2014) 2818–2824.
- [31] D.K. Davies, J. Phys. D Appl. Phys. 2 (1969) 1533.
- [32] C. Zhang, W. Tang, C.B. Han, F.R. Fan, Z.L. Wang, Adv. Mater. 26 (2014) 3580–3591.
- [33] Z.L. Wang, Mater. Today 20 (2017) 74–82.



Lingxiao Gao received the M.S. degree from the Chongqing University in 2014. She is currently a Ph.D. candidate under the supervision of Prof. Xiaojing Mu at Chongqing University, China. Her research interest mainly includes the synthesis of flexible films and energy harvester.



Tingting Wang is an engineer of unmanned underwater vehicles (UUVs) at China Academy of Aerospace Aerodynamics (CAAA). She obtained her master degree from Beihang University at 2017. Her research interests include guidance navigation and control (GNC), technology of ocean energy application of UUVs.



Lu Shan received the M.S. degree from the Chongqing University of China, Chongqing, in 2016. He is currently pursuing the Ph.D. degree at the Key Laboratory of Optoelectronic Technology & Systems Ministry of Education, International R & D center of Micro-nano Systems and New Materials Technology, Chongqing University, Chongqing, China. His research interests mainly include self-powered sensor, energy harvester and its power management.



Aobo Wang is an engineer of unmanned underwater vehicle (UUV) at China Academy of Aerodynamics(CAAA). He obtained his master degree of Ship Building and Ocean Engineering from Harbin Engineering University at 2015. His research interests include design and application of modular UUV, autonomous recovery, energy system of UUV.



Weibo Xie received the M.S. degree from the Harbin Engineering University in 2014. He is currently a Ph.D. candidate under the supervision of Prof. Zhijiang Xie at Chongqing University, China. His research interests mainly focus on the intelligent manufacturing technology.



Caiqian Yue is a senior engineer of unmanned underwater vehicles (UUVs) at China Academy of Aerospace Aerodynamics (CAAA). He obtained his master degree from Tian Jin University. He specializes in fluid mechanics and has been responsible for the key technology research of multiple UUVs



Xin Chen received the M.S. degree from the School of Measurement and Communication at Harbin University of Science & Technology, China, in 2018. She is currently pursuing the Ph. D. under the supervision of Prof. Xiaojing Mu at Chongqing University, China. Her research interests focus on FSI energy harvester.



Daqiao Tong received the B.E. degree from the School of Shenyang University of Technology, China, in 2019. He is currently pursuing the M.S. degree under the supervision of Prof. Xiaojing Mu at Chongqing University, China. His research interests focus on FSI energy harvester.



Dr. Liangke Wu is currently a lecturer affiliated with College of Aerospace Engineering, Chongqing University. He received his Ph.D. degree in mechanical engineering from Zhejiang University in 2015. His research interests include piezoelectric composites and the energy harvesting technology. He has published over 10 SCI journal papers in the related field.



Wenqian Lei received the B.S. degree from Chongqing University of China, in 2019. She is currently pursuing the Master degree at Chongqing University. Her research interest is the energy management circuit.



Prof. Hua Yu received his Ph.D in 2006 from Huazhong University of Science & Technology, China. He is currently a professor in Chongqing University, China. His main research interests focus on the MEMS, energy harvesting, IC design and self-powered sensor.



Prof. Zhong Lin (ZL) Wang received his Ph.D. from Arizona State University in physics. He now is the Hightower Chair in Materials Science and Engineering, Regents' Professor, Engineering Distinguished Professor and Director, Center for Nanostructure Characterization, at Georgia Tech. Dr. Wang has made original and innovative contributions to the synthesis, discovery, characterization and understanding of fundamental physical properties of oxide nanobelts and nanowires, as well as applications of nanowires in energy sciences, electronics, optoelectronics and biological science. His discovery and breakthroughs in developing nanogenerators established the principle and technological road map for harvesting mechanical energy from environment and biological systems for powering a personal electronics. His research on self-powered nanosystems has inspired the worldwide effort in academia and industry for studying energy for micro-nano-systems, which is now a distinct disciplinary in energy research and future sensor networks. He coined and pioneered the field of piezotronics and piezophotonics by introducing piezoelectric potential gated charge transport process in fabricating new electronic and optoelectronic devices. Details can be found at: <http://www.nanoscience.gatech.edu>.



Dr. Xiaobin He received the B.E. degree from Nanchang University of China, in 1999, and received his Ph.D from Shanghai Jiao Tong University in 2009. Now he is a boffin in the Shanghai Academy of Spaceflight Technology, Shanghai Institute of Space Power Source, Shanghai. His main research interests focus on the space power source.



Prof. Xiaojing Mu is currently a full professor affiliated with College of Optoelectronic Engineering, Chongqing University. He is also the deputy executive director of "Defense Key Disciplines Lab of Novel Micro-nano Devices and System Technology" in Chongqing University. He received his Ph.D. degree in mechanical engineering from the National University of Singapore in 2013, and worked as a research scientist from 2013-2015 in Institute of Microelectronics (IME), A*STAR, Singapore. His research interests include energy harvester, Surface Acoustic Wave (SAW) sensor/filter, and M/NEMS technologies. He has published over 70 SCI journal papers, and authorized/applied 40 patents, including 4 international patents.



Prof. Ya Yang received his Ph.D. in Materials Science and Engineering from University of Science and Technology Beijing, China. He is currently a professor at Beijing Institute of Nanoenergy and Nanosystems, Chinese Academy of Sciences, China. He has developed various new hybridized and multi-effects coupled nanogenerators, opening up the new principles of the device design and coupled effects, and the new approaches of improving output performances of energy-related devices. His main research interests focus on the field of hybridized and coupled nanogenerators for energy conversion, self-powered sensing, and some new physical effects.